

# Cadherin 26 is an alpha integrin-binding epithelial receptor regulated during allergic inflammation

JM Caldwell<sup>1</sup>, MH Collins<sup>2</sup>, KA Kemme<sup>1</sup>, JD Sherrill<sup>1</sup>, T Wen<sup>1</sup>, M Rochman<sup>1</sup>, EM Stucke<sup>1</sup>, L Amin<sup>1</sup>, H Tai<sup>1</sup>, PE Putnam<sup>3</sup>, MJ Jiménez-Dalmaroni<sup>4</sup>, MR Wormald<sup>5</sup>, A Porollo<sup>6</sup>, JP Abonia<sup>1</sup> and ME Rothenberg<sup>1</sup>

Cadherins (CDH) mediate diverse processes critical in inflammation, including cell adhesion, migration, and differentiation. Herein, we report that the uncharacterized cadherin 26 (CDH26) is highly expressed by epithelial cells in human allergic gastrointestinal tissue. *In vitro*, CDH26 promotes calcium-dependent cellular adhesion of cells lacking endogenous CDHs by a mechanism involving homotypic binding and interaction with catenin family members (alpha, beta, and p120), as assessed by biochemical assays. Additionally, CDH26 enhances cellular adhesion to recombinant integrin  $\alpha 4\beta 7$  *in vitro*; conversely, recombinant CDH26 binds  $\alpha E$  and  $\alpha 4$  integrins in biochemical and cellular functional assays, respectively. Interestingly, CDH26-Fc inhibits activation of human CD4<sup>+</sup> T cells *in vitro* including secretion of IL-2. Taken together, we have identified a novel functional CDH regulated during allergic responses with unique immunomodulatory properties, as it binds  $\alpha 4$  and  $\alpha E$  integrins and regulates leukocyte adhesion and activation, and may thus represent a novel checkpoint for immune regulation and therapy via CDH26-Fc.

## INTRODUCTION

Cadherins (CDHs), a family of transmembrane cell surface glycoproteins, mediate calcium-dependent cell adhesion and exhibit a tightly regulated tissue-specific expression pattern. CDHs expressed predominantly within epithelia such as E-cadherin (CDH1) and P-cadherin (CDH3)<sup>1</sup> contribute to the maintenance of skin and mucosal barriers, regulating access of pathogens and allergens to underlying tissue and immunocytes. Modulation of CDH expression and function has been associated with a number of diseases such as cancer, in which metastatic tumorigenesis is often associated with a switch in CDH expression such as CDH1 to CDH2 (N-cadherin),<sup>2</sup> as well as diverse inflammatory diseases, including but not limited to asthma, eczema, chronic rhinosinusitis, inflammatory bowel disease, and rheumatoid arthritis.<sup>3–7</sup> Focusing on epithelial CDHs, reduced CDH1 occurs in gastroesophageal reflux disease, asthma, and eczema and has been shown to contribute to loss of epithelial integrity, impairment of barrier function, and production of pro-inflammatory cytokines.<sup>6,8–10</sup> A

substantial advance in the CDH field has been the finding that CDH1 binds lymphocyte integrin  $\alpha E\beta 7$  and regulates the activation and localization of epidermal and intestinal intraepithelial lymphocytes.<sup>11–14</sup> Despite these observations regarding CDH1, the involvement of other CDHs in the regulation of immunological processes mediated by the mucosal epithelium, such as their binding to integrins, has not been described.

Allergic disorders are characterized by a T helper type 2 (Th2) immune response that involves the accumulation of distinct subsets of activated leukocytes at the affected site. In particular, in addition to eosinophils, increased numbers of CD4<sup>+</sup> T cells and type 2 innate lymphoid cells have been observed at sites of allergic gastrointestinal (GI) inflammation.<sup>15–18</sup> Furthermore, highly elevated levels of Th2 cytokines, including interleukin (IL)-13, suggest activation of these cells at sites of allergic GI inflammation.<sup>19,20</sup> In general, it is known that leukocytes, in part under the influence of soluble mediators including cytokines and chemokines, localize from the blood to tissue in a multi-step process involving the coordinate

<sup>1</sup>Division of Allergy and Immunology, Cincinnati Children's Hospital Medical Center, University of Cincinnati College of Medicine, Cincinnati, Ohio, USA. <sup>2</sup>Division of Pathology and Laboratory Medicine, Cincinnati Children's Hospital Medical Center, University of Cincinnati College of Medicine, Cincinnati, Ohio, USA. <sup>3</sup>Division of Gastroenterology, Hepatology and Nutrition, Cincinnati Children's Hospital Medical Center, University of Cincinnati College of Medicine, Cincinnati, Ohio, USA. <sup>4</sup>Department of Biological Chemistry, John Innes Centre, The Sainsbury Laboratory, Norwich, UK. <sup>5</sup>The Glycobiology Institute, Department of Biochemistry, University of Oxford, Oxford, UK and <sup>6</sup>Center for Autoimmune Genomics and Etiology, Division of Biomedical Informatics, Cincinnati Children's Hospital Medical Center, University of Cincinnati College of Medicine, Cincinnati, Ohio, USA. Correspondence: ME Rothenberg (Rothenberg@cchmc.org)

Received 6 July 2016; accepted 10 November 2016; published online 4 January 2017. doi:10.1038/mi.2016.120

expression and activation of leukocyte-expressed selectins and integrins and their counter-receptors on activated endothelium.<sup>21</sup> However, less is known about how leukocyte-expressed receptors interact with epithelial ligands to influence cellular localization and activation, particularly in the context of allergic inflammation.

We identified a previously uncharacterized CDH-like molecule, CDH26, that was markedly overexpressed in human GI tissue with active eosinophilic inflammation.<sup>20</sup> No studies of this molecule have been reported, although its transcript appears to be upregulated in epithelial cells under Th2-associated conditions.<sup>22–25</sup> Herein we demonstrate that CDH26 is a unique functional CDH, in that it (1) has an epithelial cell-restricted expression pattern that is particularly prominent following gene induction during allergic inflammation; (2) is an  $\alpha 4$  and  $\alpha E$  integrin receptor; (3) has the capacity to modulate leukocyte adhesion and activation; and (4) has immunomodulatory function that can be exploited via a CDH26-Fc fusion protein, which has immunosuppressive activity.

## RESULTS

### CDH26 is overexpressed during pathological allergic inflammation

Gastric tissue of control patients and patients with an allergic gastroenteropathy, eosinophilic gastritis (EG), was subjected to global transcript analysis.<sup>20</sup> Additional information about these patients can be found in **Supplementary Methods** and **Supplementary Table S2** online. We identified that the most upregulated transcript that passed the criteria  $P < 0.01$  and 2-fold filter was the uncharacterized CDH family member cadherin 26 (*CDH26*) (12.3-fold,  $P < 0.005$ ).<sup>20</sup> We verified by real-time PCR analysis that the *CDH26* mRNA level was highly increased in the gastric tissue of EG patients within the same cohort subjected to microarray (15.3-fold,  $n = 5$  EG vs.  $n = 5$  control,  $P = 0.03$ ; see **Supplementary Figure S1a**) as well as in additional EG patient gastric tissue (35.6 fold,  $n = 10$  EG vs.  $n = 10$  control,  $P < 0.0001$ ; see **Supplementary Figure S1b**). Comparison of the genes differentially regulated in EG<sup>20</sup> and in eosinophilic esophagitis (EoE)<sup>26</sup> revealed that *CDH26* was the only CDH family member that exhibited a significant change in gene expression in both allergic disorders. Indeed, as previously observed,<sup>19</sup> *CDH26* mRNA expression was significantly increased (115-fold) in the esophageal tissue of patients with active EoE compared with control patients (**Figure 1a**). Only *CDH1* (E-cadherin) and *CDH26* exhibited raw signals indicative of the transcripts being substantially expressed (i.e., at least one sample for that probe exhibited raw signal  $\geq 400$ ) in the gastric tissue of patients with active EG (**Figure 1b**). Raw signals for CDH transcripts in esophageal tissue from EoE patients only showed such values for *CDH1*, *CDH3* (P-cadherin), and *CDH26* (**Figure 1c**). As a control, no significant change in *CDH26* or *CCL26* (eotaxin-3) expression was observed in gastric tissue of patients with *Helicobacter pylori* gastritis compared with control patients, although control C3 transcript was elevated in the *H. pylori* cohort

as previously reported (**Figure 1d** and Ikuse *et al.*<sup>27</sup> and Wen *et al.*<sup>28</sup>). Notably, a microarray study of gastric antrum tissue of patients with *H. pylori* gastritis did not identify *CDH26* as being upregulated compared with normal tissue.<sup>27</sup> Thus, *CDH26* is a unique CDH in terms of its expression level and regulation in two distinct allergic states.

### CDH26 protein expression is increased in inflamed allergic GI tissue and is localized to epithelial cells

Immunohistochemical staining for CDH26 showed localization nearly exclusively in the surface and gland epithelial cells in gastric tissue of patients with EG (**Figure 2a,b**). The mean peak number of CDH26-positive cells was 241 cells/ $\times 400$  high-power field (mean  $\pm$  s.e.m.,  $104.2 \pm 40.8$ ;  $P = 0.0476$ , Mann-Whitney test) in EG patients compared with no expression above background in controls. Western blotting revealed an increased level of gastric CDH26 (4.9-fold) in EG patients compared with control samples (**Figure 2c**). Patients with active EoE had high levels of esophageal CDH26 protein expression compared with control patients. In control esophageal biopsies, the staining was confined to epithelial cells near the surface, but in active EoE the staining was both more intense and prevalent and included both surface epithelial cells and epithelial cells in the expanded basal layer (**Figure 2d**). By western blotting analysis, esophageal tissue of EoE patients showed 3.4-fold increased CDH26 protein levels compared with control tissue (**Figure 2e**).

### CDH26 is a functional CDH

CDH26 exhibits sequence homology to the CDH family of proteins, with five extracellular CDH repeats<sup>29</sup> in the putative extracellular portion of the protein, a predicted transmembrane domain, and a C-terminal cytoplasmic region (**Figure 3a**). To determine whether CDH26 localized to the cell membrane of esophageal epithelial cells, affinity isolation of biotinylated surface proteins was performed. Proteins present on the surface of cells were labeled with biotin, the cells were lysed and proteins solubilized, and biotinylated proteins were subjected to affinity isolation using streptavidin beads. Proteins bound to the streptavidin beads were subsequently solubilized in loading buffer and subjected to sodium dodecyl sulfate–polyacrylamide gel electrophoresis (SDS–PAGE). Western blotting for CDH26 indicated that it was present at the cell surface in esophageal epithelial cells that express high levels of CDH26 (**Figure 3b**) because it was pulled down only from cells overexpressing CDH26 that underwent surface biotinylation (**Figure 3b**, lane 8).

CDH26 contains five asparagine residues in its extracellular domain; these residues are located within the consensus sequence for N-linked glycosylation (N81, N85, N171, N177, N462). To test whether CDH26 is modified by N-linked glycosylation, CDH26 was immunoprecipitated and then treated with peptide: N-glycosidase F (PNGase F) that was either active or heat-inactivated as a negative control. The treated, immunoprecipitated proteins were then subjected to SDS–PAGE and western blotting analysis for CDH26. Immunoprecipitated CDH26 treated with peptide: N-glycosidase

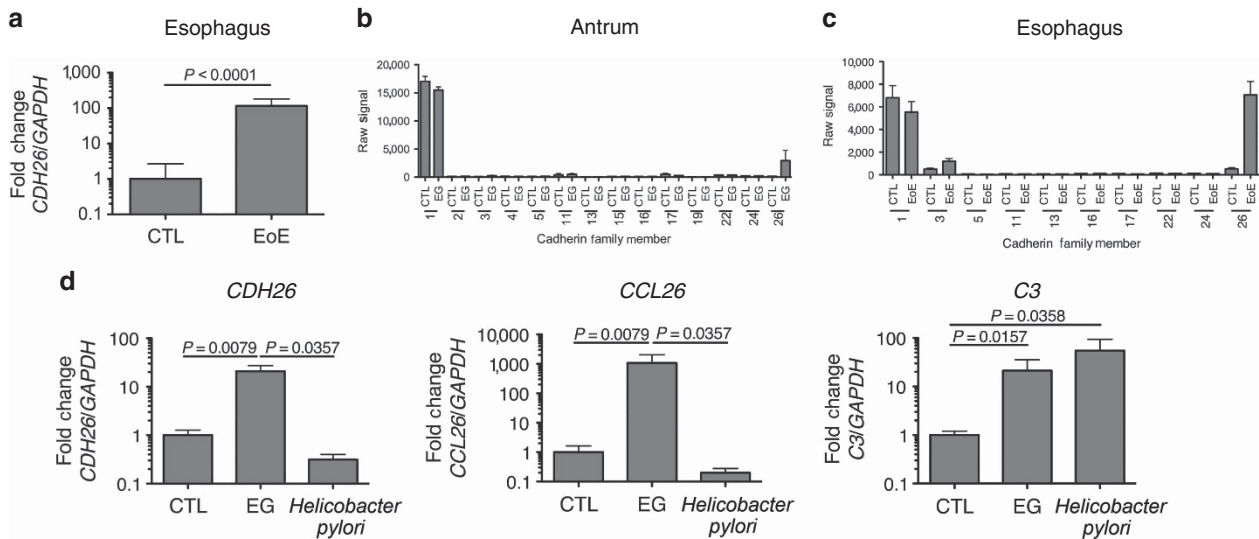


**Figure 1** Cadherin 26 (*CDH26*) expression in allergic tissue. **(a)** Relative esophageal tissue *CDH26* transcript levels were determined ( $n = 66$  control (CTL),  $n = 77$  eosinophilic esophagitis (EoE) patients). The bars represent the median, and the error bars represent the interquartile range **(b and c)**. The mean raw expression value (bars) for each cadherin probe in which any patient sample exhibited a signal intensity  $> 100$  is graphed for **(b)** the gastric tissue of 5 CTL and 5 eosinophilic gastritis (EG) patients<sup>20</sup> or for **(c)** the esophageal tissue of 14 CTL and 18 EoE patients characterized previously.<sup>26</sup> For each cadherin, only the probe with the highest raw signal is shown. For **(b and c)**, error bars represent the s.e.m. **(d)** Relative *CDH26*, *CCL26* (eotaxin-3), and *C3* transcript levels from the gastric antrum tissue of CTL patients ( $n = 5$ ), EG patients ( $n = 5$ ), and *H. pylori* gastritis patients ( $n = 3$ ) were determined. The bars represent the mean, and error bars represent the s.e.m. For **(a and d)**, data were analyzed by Mann–Whitney test.

F (PNGase F) (**Figure 3c**, lane 5), but not heat-inactivated PNGase F (**Figure 3c**, lane 6), exhibited increased mobility compared with CDH26 from total cell lysates, indicating that the protein is modified by *N*-linked glycosylation under baseline conditions.

CDH26 contains a tryptophan residue at position 2 of the most N-terminal extracellular CDH repeat domain known to be critical for dimerization *in trans* of type I and type II CDHs.<sup>30</sup> Therefore, we tested whether CDH26 molecules interact in a homotypic manner. When co-expressed, myc-tagged CDH26 co-immunoprecipitated with hemagglutinin (HA)-tagged CDH26 (**Figure 3d**, lane 7), and the reciprocal immunoprecipitation (IP) confirmed that CDH26–HA co-immunoprecipitated with CDH26–MYC (**Figure 3d**, lane 8).

We next tested whether CDH26 interacted with beta-catenin, which binds other CDH molecules to link them indirectly to the actin cytoskeleton.<sup>30–32</sup> The region of CDH1 known to interact with beta-catenin exhibited 68% similarity to the same region of CDH26 (Stappert and Kamler<sup>31</sup> and Jou *et al.*<sup>32</sup>, see **Supplementary Figure S2a,b,d**). When IP of HA-tagged beta-catenin was performed, CDH26 was also detected in the precipitates (**Figure 3e**, lanes 7 and 9), indicating that beta-catenin and CDH26 exist in the same complex.

Beta-catenin interacts with alpha-catenin to link CDH molecules indirectly to the actin cytoskeleton and thus support cell adhesion.<sup>30</sup> We tested whether alpha-catenin exists in the same complex as CDH26 and found that CDH26 co-immunoprecipitated with alpha-catenin (**Figure 3f**, lane 6). As a positive control, beta-catenin was also observed to co-immunoprecipitate with alpha-catenin (**Figure 3f**, lane 6).

p120-catenin binds the juxtamembrane domain of the cytoplasmic portion of CDH molecules and has been shown

to function in the maintenance of CDH stability and localization to the cell surface.<sup>30</sup> The primary amino-acid sequence of the juxtamembrane domain of CDH1 was notably homologous (48%) to that in CDH26 (see **Supplementary Figure S2a,c,d**). We therefore tested whether CDH26 and p120-catenin could exist in the same protein complex and found that p120-catenin and CDH26 co-immunoprecipitated (**Figure 3g**, lane 9).

We tested whether CDH26 could promote calcium-dependent cellular adhesion. To do this, L929 cells, which lack endogenous CDHs, were used in an aggregation assay. L929 cells that were transduced with a CDH26 expression construct and thus expressed high levels of CDH26 showed a high degree of aggregation only in the presence of calcium (**Figure 3h**, column 4 vs. column 3), whereas cells transduced with a control expression construct aggregated neither in the presence nor in the absence of calcium (**Figure 3h**, columns 1 and 2).

### CDH26 binds $\alpha 4$ and $\alpha E$ integrins

Heterotypic binding of CDHs and integrins has been reported.<sup>12,33</sup> There are a number of proteins known to bind integrins, including CDH1 as well as ICAM-1 (intercellular adhesion molecule 1), MAdCAM-1 (mucosal addressin cell adhesion molecule 1), and fibronectin, for which 3D structures have been resolved and integrin-binding sites have been localized.<sup>34</sup> To map these sites to CDH26, we generated a 3D model of CDH26 structure using homology modeling with the CDH1 structure (PDB ID 3Q2V) as a primary template. The pairwise structure alignment of the model (blue) with other resolved structures (gray) indicates putative integrin-binding sites in CDH26 (**Figure 4a**). As can be seen, known integrin-binding sites are located in the unstructured loops of



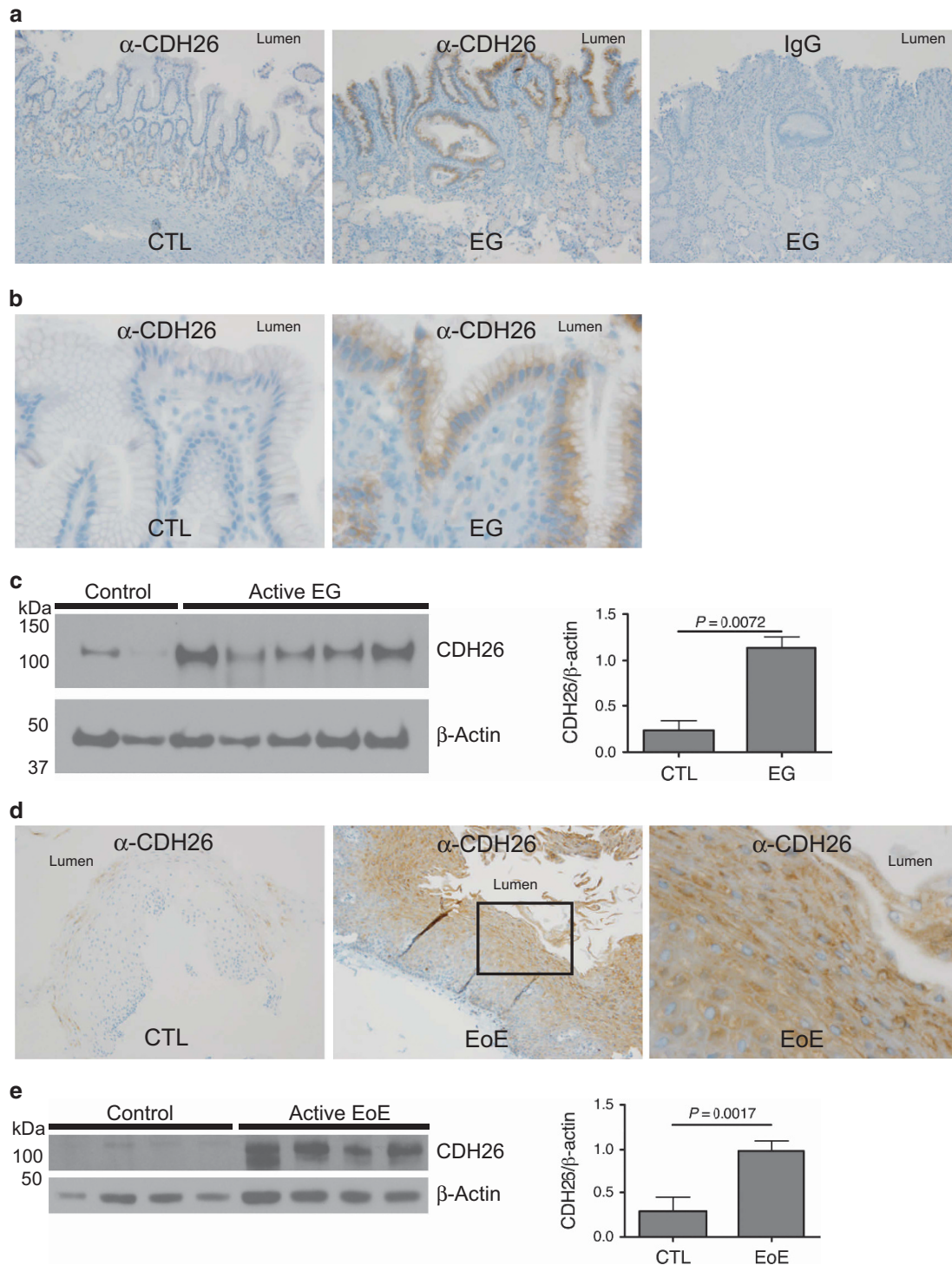


**Figure 2** Cadherin 26 (CDH26) expression and localization in epithelial cells in allergic gastrointestinal tissue. **(a)** Representative control (CTL) and eosinophilic gastritis (EG) patient gastric biopsy specimen ( $\times 200$ ) stained with anti-CDH26 antibody or control immunoglobulin G (IgG). **(b)** CTL and EG biopsy specimen ( $\times 800$ ) stained with anti-CDH26 antibody. **(c)** Left: Gastric antrum protein lysates were subjected to sodium dodecyl sulfate–polyacrylamide gel electrophoresis (SDS–PAGE) and western blotting analysis. Right: The ratio of CDH26 to beta-actin signal was graphed; bars represent the mean, and error bars represent the s.e.m. **(d)** Immunohistochemical staining for CDH26 was performed on esophageal biopsy specimens ( $n = 7$  CTL,  $n = 3$  EoE). Representative CTL and EoE biopsies are shown ( $\times 200$ ,  $\times 800$  inset). **(e)** Left: Esophageal protein lysates ( $n = 4$  CTL,  $n = 4$  EoE) were subjected to SDS–PAGE and western blotting analysis. Right: The ratio of CDH26 to beta-actin signal was graphed; bars represent the mean, and error bars represent the s.e.m. For **c** and **e**, data were analyzed by unpaired *t*-test. For **(a, b, and d)**, the location of the lumen is denoted to facilitate interpretation of the orientation of the tissue section.

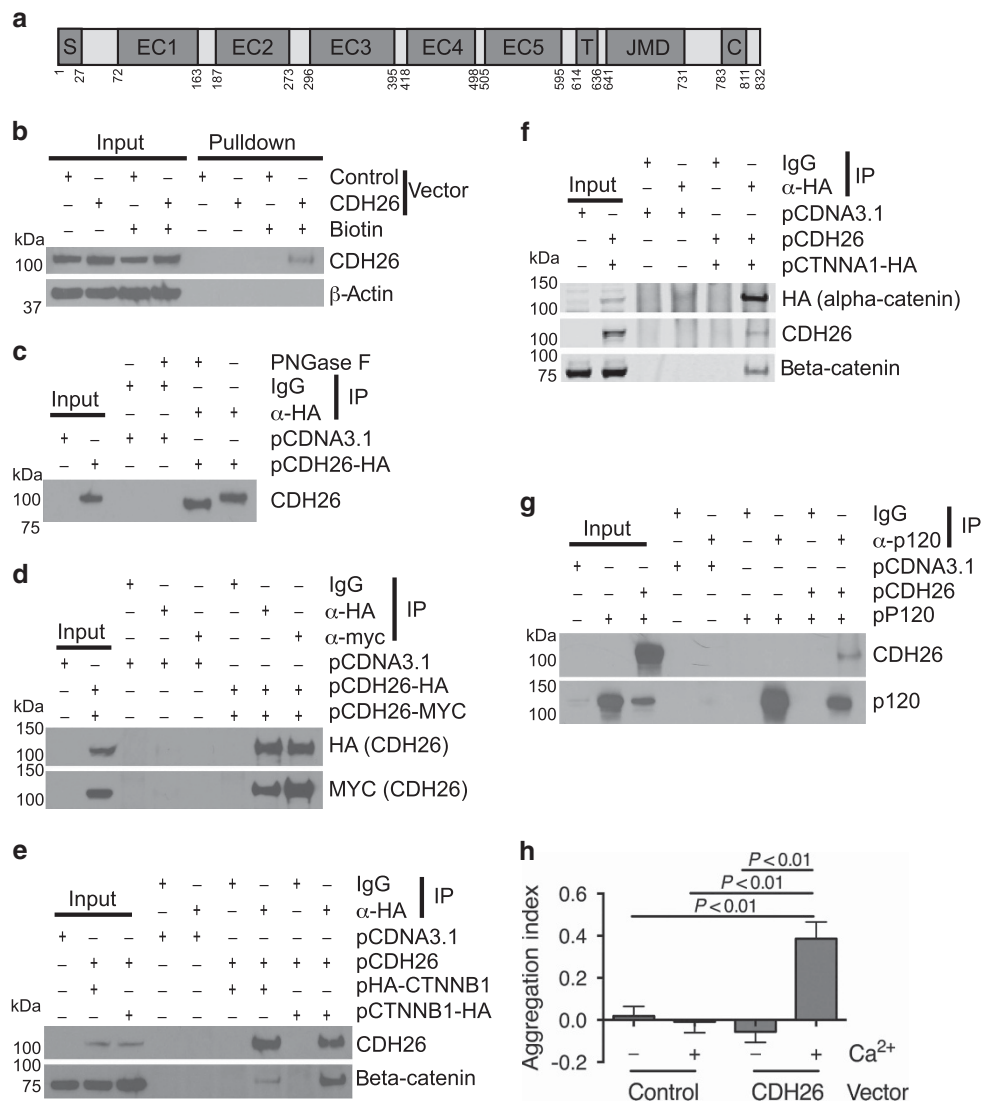


**Figure 3** Biochemical and functional properties of cadherin 26 (CDH26). **(a)** Schematic representing human CDH26 domain structure. S: signal peptide, EC1–EC5: extracellular cadherin repeat 1–5, T: transmembrane domain, JMD: juxtamembrane domain, C: CBD, catenin-binding domain. **(b)** Surface biotinylation of TE-7 cells. Cell surface proteins were labeled with biotin and pulled down with streptavidin beads. Total cell lysates (input) and proteins bound to the streptavidin beads were subjected to sodium dodecyl sulfate–polyacrylamide gel electrophoresis (SDS–PAGE) and western blotting analysis. Predicted CDH26 molecular weight: 92.4 kDa. **(c)** Immunoprecipitates from transiently transfected HEK 293T cells were treated with either peptide: *N*-glycosidase F (PNGase F) (+) or heat-inactivated PNGase F (–). Inputs (1/10 of amount used for immunoprecipitation (IP)) and treated immunoprecipitates were subjected to SDS–PAGE and western blotting analysis. Each blot shown is representative of three independent experiments. **(d–g)** Immunoprecipitates from transiently transfected HEK 293T cells and inputs (1/10 of amount used for IP) were subjected to SDS–PAGE and western blotting analysis. Each blot shown is representative of three independent experiments. **(h)** Transduced L929 cells were dispersed, incubated in buffer either containing or lacking 1 mM CaCl<sub>2</sub>, and assessed for the degree of aggregation. Bars represent the mean, and error bars represent the s.e.m. Data show one experiment representative of three and were analyzed by one-way analysis of variance followed by Tukey's posttest.

extracellular domain and are negatively charged. D42 of MADCAM-1 and E34 of ICAM-1 overlap with D98, E99, and E102 in CDH26. D1495 of fibronectin corresponds to E138 of CDH26. The presence of these negatively charged residues in the unstructured loops on the surface suggests that CDH26 would bind integrins.

We tested whether L929 cells expressing high levels of CDH26 exhibited adhesion to  $\alpha$ 4 $\beta$ 7 compared with control cells. Indeed, L929 cells transduced with a CDH26 expression vector showed increased adhesion to  $\alpha$ 4 $\beta$ 7-coated wells compared with control cells, in contrast to bovine serum

albumin (BSA)-coated wells, which did not support adhesion of either cell type (**Figure 4b**). Visualization of cellular binding revealed a marked increase of CDH26-expressing cells binding  $\alpha$ 4 $\beta$ 7 (**Figure 4c**). To further prove that CDH26 could directly bind  $\alpha$ 4 $\beta$ 7, a solid-phase adhesion assay was performed in which recombinant CDH26-hIgG1-Fc (referred to as CDH26-Fc hereafter; see **Supplementary Figure S3** and **Supplementary Methods** for details of isolation) was added to wells that were coated with recombinant  $\alpha$ 4 $\beta$ 7. CDH26-Fc bound specifically to  $\alpha$ 4 $\beta$ 7 and not BSA, whereas negative control IgG did not bind either  $\alpha$ 4 $\beta$ 7 or BSA (**Figure 4d**).

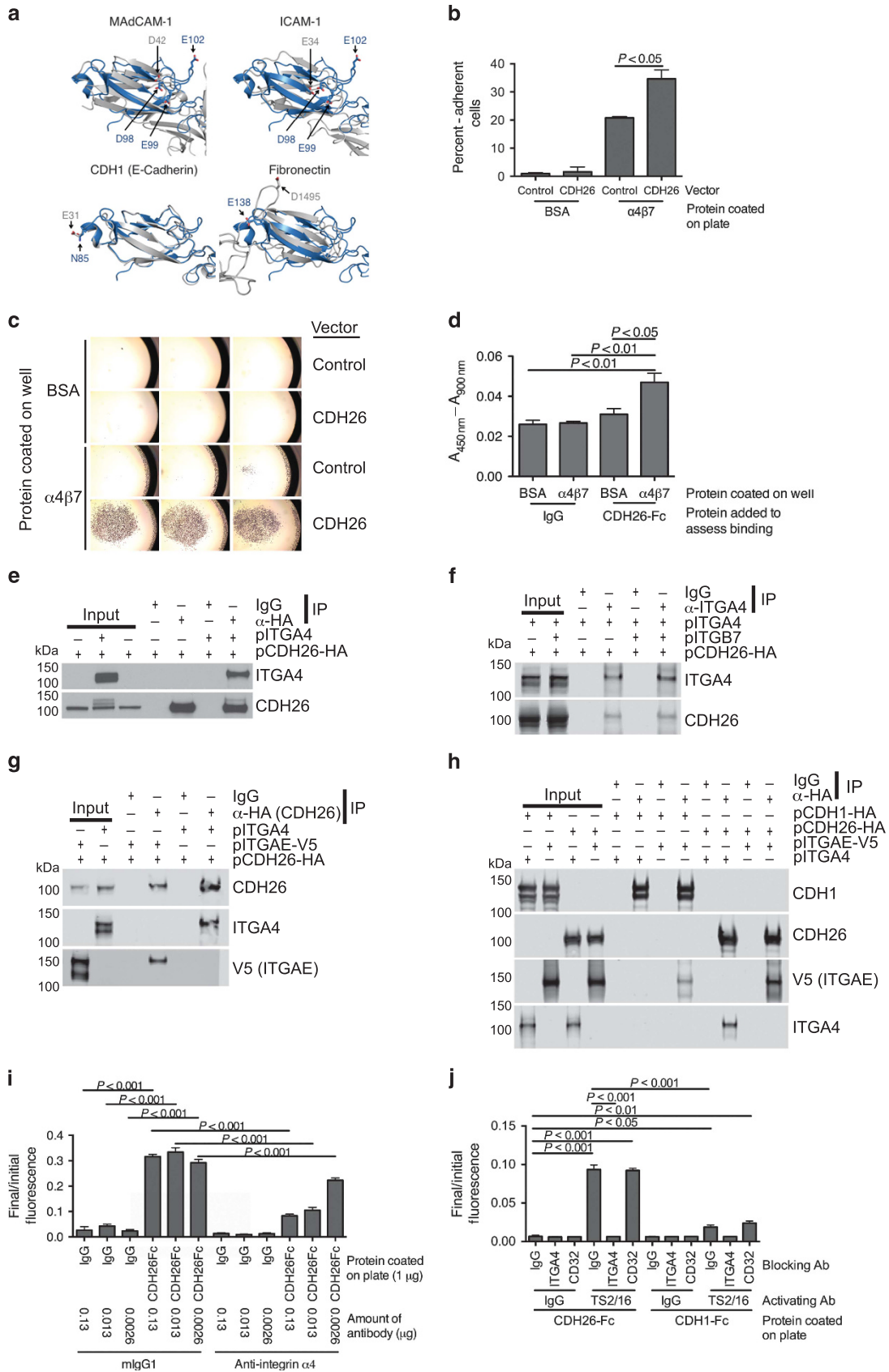


**Figure 4** For caption see page 1196.

**Figure 4** Binding of cadherin 26 (CDH26) to integrins. **(a)** Pairwise structure alignment of CDH26 with known integrin ligands. CDH26 structure was modeled (blue) and aligned to the resolved structures of MAdCAM-1 (mucosal addressin cell adhesion molecule 1; PDB ID 1BQS), ICAM-1 (intercellular adhesion molecule 1; PDB ID 1IC1), CDH1 (PDB ID 1EDH), and fibronectin (PDB ID 1FNF) (gray). For each pair, integrin-binding amino acids and the corresponding CDH26 residues are labeled (arrows) and rendered using a stick representation. **(b)** Transduced L929 cell clones were dispersed and added to wells coated with either bovine serum albumin (BSA) or recombinant  $\alpha 4\beta 7$ . The percentage of adherent cells remaining after wells were washed is shown. The graph represents seven experiments combined that each involved separate control and CDH26-overexpressing clones. **(c)** Pictures of Giemsa-stained wells from **b** were taken (original magnification,  $\times 4$ ), with one control and one CDH26-overexpressing clone shown. **(d)** Wells were coated with or without recombinant  $\alpha 4\beta 7$  and then blocked with BSA, followed by addition of either hlgG1 or CDH26-hlgG1-Fc (CDH26-Fc). Bound antibody or fusion protein was then detected and expressed as  $A_{450\text{nm}} - A_{900\text{nm}}$ . Each condition was performed in triplicate. This graph shows one experiment representative of three. **(e–h)** Inputs (1/10 of amount used for immunoprecipitation) and immunoprecipitates from transiently transfected HEK 293T cells were subjected to sodium dodecyl sulfate–polyacrylamide gel electrophoresis and western blotting analysis. Each blot shown is representative of three independent experiments. **(i, j)** Fluorescently labeled Jurkat cells (untreated **(i)** or incubated with TS2/16 integrin  $\beta 1$ -activating antibodies **(j)**) preincubated with the indicated amount of control mlgG1, anti-integrin  $\alpha 4$  (HP2/1), or anti-CD32 antibodies were added to wells coated with control hlgG1, CDH26-hlgG1-Fc (CDH26-Fc), or CDH1-hlgG1-Fc (CDH1-Fc), as indicated. The graph indicates the percentage of fluorescence remaining after wells were washed. For **b, d, i, and j**, bars represent the mean, error bars represent the s.e.m, and data were analyzed by one-way analysis of variance followed by Tukey's posttest.

To further substantiate and address the specificity and molecular requirements for CDH26/ $\alpha 4\beta 7$  interaction, overexpression and co-IP studies were carried out using HEK 293T cells. When HA-tagged CDH26 (CDH26-HA) and integrin  $\alpha 4$  were overexpressed in HEK 293T cells, integrin  $\alpha 4$  co-immunoprecipitated with CDH26-HA (**Figure 4e**), and the reciprocal was observed as CDH26-HA was found to co-immunoprecipitate with integrin  $\alpha 4$  (**Figure 4f**). In addition to integrin  $\alpha 4$ , V5-tagged integrin  $\alpha E$  (ITGAE-V5) was observed to co-immunoprecipitate with CDH26-HA (**Figure 4g**). Integrin  $\alpha 4$  did not co-immunoprecipitate with CDH1, although positive control integrin  $\alpha E$  co-immunoprecipitated with CDH1 (**Figure 4h**).

We next tested whether  $\alpha 4$  bound to integrin  $\beta 1$  could mediate interaction with CDH26 by observing whether cells that express integrin  $\alpha 4\beta 1$  adhered to recombinant CDH26-Fc. Jurkat cells, which express integrin  $\alpha 4\beta 1$  but not  $\alpha 4\beta 7$ ,<sup>35</sup> adhered to CDH26-Fc to a significantly greater degree than they adhered to IgG control antibody (**Figure 4i**). Preincubation of Jurkat cells with anti-integrin  $\alpha 4$  antibody (HP2/1), but not an equivalent amount of control mlgG1, blocked their binding to CDH26-Fc in a dose-dependent manner (**Figure 4i**). Jurkat cells stimulated with antibodies that activate integrin  $\beta 1$  (clone TS2/16) adhered to CDH26-Fc in an integrin  $\alpha 4$ -dependent manner to a greater degree than they adhered to CDH1-Fc (**Figure 4j**).

### CDH26 modulates CD4<sup>+</sup> T-cell activation

Because other  $\alpha 4\beta 1$  ligands, including VCAM-1 (vascular cell adhesion molecule 1), have been shown to co-stimulate CD4<sup>+</sup> T-cell activation,<sup>36–38</sup> we sought to test the hypothesis that the putative integrin  $\alpha 4$  ligand CDH26 had this property. After human peripheral blood CD4<sup>+</sup> T cells isolated by negative selection (detailed in **Supplementary Methods**) were incubated for 48 h in the presence of plate-bound anti-CD3 antibodies (clone OKT3) to induce suboptimal stimulation of the T-cell receptor (TCR), an increased percentage of the cells expressed CD25 at the cell surface as assessed by flow cytometric analysis (detailed in **Supplementary Methods**). However, the presence of CDH26-Fc, but not IgG control, inhibited the increase in percentage of cells expressing CD25 in a dose-dependent manner (**Figure 5a**; see **Supplementary**

**Figure S4a**). Likewise, production of the cytokine IL-2 was inhibited by CDH26-Fc in a dose-dependent manner in cells subjected to TCR stimulation (**Figure 5b**). A similar inhibition of IL-4 secretion and CD69 and CD154 surface expression were also observed (data not shown). We next tested whether this effect was specific to CDH26-Fc or whether other cadherin-Fc proteins mediated inhibition of T-cell activation. Both CDH26-Fc and CDH1-Fc attenuated the increase of CD25 surface expression following TCR stimulation of CD4<sup>+</sup> T cells (**Figure 5c**; see **Supplementary Figure S4b**). The inhibition of CD4<sup>+</sup> T-cell activation by both cadherin-Fc constructs was also apparent at the level of cytokine secretion; cadherin-Fc constructs inhibited the secretion of IL-2 in response to TCR stimulation (**Figure 5d**).

### DISCUSSION

Herein we have elucidated the properties of CDH26, identifying it as a functional CDH with unique features in that it is the only CDH family member significantly upregulated in human allergic GI tissue, where it localizes to epithelial cells in the inflamed esophagus and stomach. CDH26 mediates calcium-dependent cell adhesion, dimerizes/multimerizes, and interacts with alpha-, beta-, and p120-catenins. CDH26 also has the ability to impact leukocyte migration and adhesion. Moreover, we present biochemical, molecular, and functional evidence that CDH26–integrin interactions impact cellular adhesion; specifically, integrins  $\alpha 4$  and  $\alpha E$  co-immunoprecipitate with CDH26, recombinant CDH26-Fc binds recombinant  $\alpha 4\beta 7$ , CDH26-expressing cells adhere to integrin  $\alpha 4\beta 7$ , and Jurkat cells adhere to recombinant CDH26-Fc in a manner dependent on integrin  $\alpha 4$  (see **Figure 6** and see **Supplementary Table S1** for summary and comparison to CDH1). Besides uncovering a novel role for this molecule, we present evidence that it can be exploited to generate a potential therapeutic as CDH26-Fc is an immunosuppressive molecule, at least *in vitro*. Taken together, we have identified a novel functional CDH regulated during allergic inflammation and determined that it binds  $\alpha$  integrins and has immunomodulatory properties.

Given our observation that CDH26 interacts with not only integrin  $\alpha 4$  but also integrin  $\alpha E$ , it might have a function similar to E-cadherin to regulate localization or activation of leukocytes during allergic responses via interacting with leukocyte



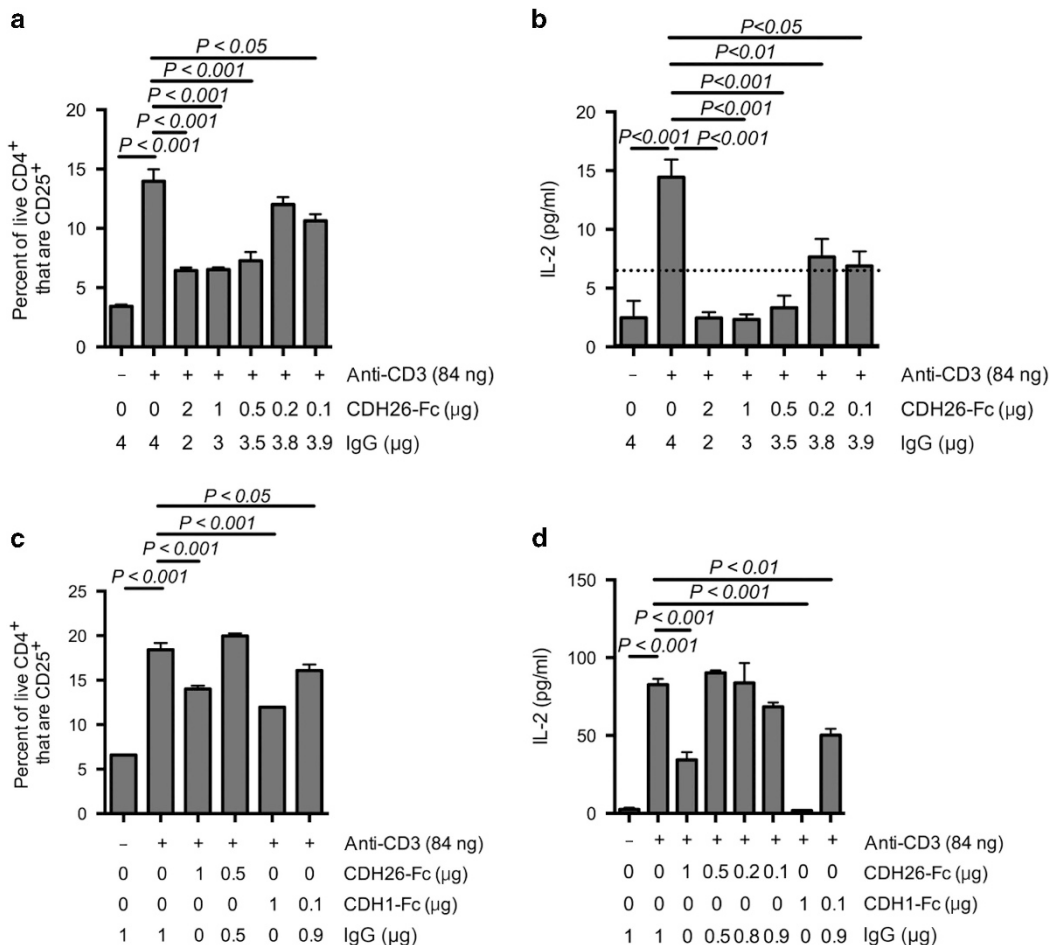


**Figure 5** Effect of cadherin 26 (CDH26)-Fc and CDH1-Fc on CD4<sup>+</sup> T-cell activation. Human peripheral blood CD4<sup>+</sup> T cells were isolated and cultured for 48 h in wells coated with the indicated amounts of proteins (IgG, anti-CD3, CDH26-Fc, and/or CDH1-Fc). Cells were stained for flow cytometric analysis to detect CD4 and CD25, and supernatants were analyzed to detect interleukin (IL)-2 levels by enzyme-linked immunosorbent assay (ELISA). For **a** and **c**, the percentage of live CD4<sup>+</sup> cells that are CD25<sup>+</sup> are shown, and for **(b and d)**, the amount of IL-2 detected in the supernatant is shown. The dotted lines represent the detection limit for the ELISA. For **(a to d)**, bars represent the mean, and error bars represent the s.e.m. Data were analyzed by one-way analysis of variance followed by Tukey's posttest. Data are results from one subject representative of those from five individual subjects for **(a and b)** and from one subject representative of those from four individual subjects for **(c and d)**.

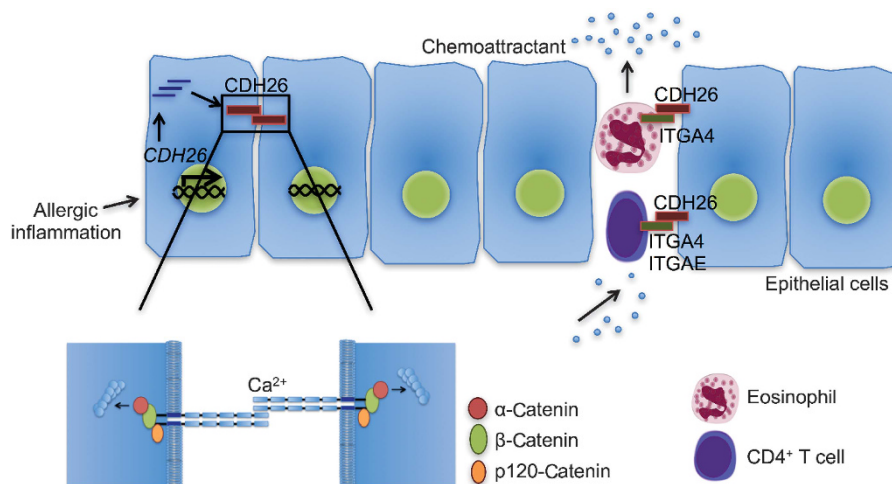


**Figure 6** Model of cadherin 26 (CDH26) expression and function in allergic inflammation. CDH26 is expressed by gastrointestinal (GI) epithelial cells in allergic GI inflammatory conditions. CDH26 dimerizes; interacts with beta-, alpha-, and p120-catenins; and mediates calcium-dependent cell adhesion. CDH26 additionally interacts with integrin  $\alpha$ 4 (ITGA4) and integrin  $\alpha$ E (ITGAE), which may impact leukocyte migration, localization, or activation status in allergic tissue.



integrins. Epithelial CDH26 may impact the localization or activation status of diverse  $\alpha 4^{+}$  and/or  $\alpha E^{+}$  cells (e.g.,  $CD4^{+}$  T cells, eosinophils, mast cells) within the epithelium in the context of allergic inflammation. In particular, these subsets of cells are known to be increased in the esophageal epithelium of EoE patients compared with control patients;<sup>17,26,39</sup> furthermore, numerous intraepithelial eosinophils are observed in EoE and EG but not in normal esophageal or gastric tissue. This altered intraepithelial localization of several subsets of cells correlates with the fact that CDH26 appears to be a highly inducible molecule in epithelial cells that is present at only low levels under homeostatic conditions.

We identified several lines of evidence that CDH26 interacts with alpha integrins and facilitates cellular binding to  $\alpha 4$ -containing integrins, including both integrin  $\alpha 4\beta 7$  and  $\alpha 4\beta 1$ . Biochemical assays suggested that the extracellular portion of CDH26 could directly bind the  $\alpha 4$ -containing integrin  $\alpha 4\beta 7$ . Furthermore, we observed that cells expressing high levels of CDH26 adhered to recombinant integrin, and in the reciprocal situation, recombinant CDH26 was sufficient to mediate adhesion of Jurkat T cells in a manner dependent on integrin  $\alpha 4$ . Such interactions are consistent with the structural properties of CDH26, which include the presence of solvent-exposed acidic residues that could be critical to facilitate the CDH26/integrin interaction. We speculate that, in addition to mediating adhesion, interaction of epithelial-expressed CDH26 with leukocyte integrins could initiate intracellular signaling in both epithelial cells and leukocytes. This could impact diverse processes, such as alteration of gene expression, regulation of barrier function, or production of mediators by either cell type.

It has been shown that integrin  $\alpha 4$  ligands, including fibronectin, VCAM-1, and MAdCAM-1, costimulate  $CD4^{+}$  T cells activated by suboptimal TCR activation.<sup>36–38</sup> Our data show that CDH26-Fc inhibited  $CD4^{+}$  T-cell activation mediated by suboptimal TCR engagement. We additionally observed that CDH1-Fc had similar effects. In fact, although CDH1 has previously been shown to co-stimulate  $CD4^{+}$  T-cell activation,<sup>40</sup> it has additionally been shown to be an inhibitory molecule in several settings; for example, ligation of E-cadherin expressed by dendritic epidermal T cells with CDH1 expressed by epidermal keratinocytes inhibits dendritic epidermal T-cell interferon- $\gamma$  production, tumor necrosis factor- $\alpha$  production, and degradation in response to TCR stimulation.<sup>14</sup> Moreover, CDH1 has been shown to be a counter-receptor for killer cell lectin-like receptor G1 (KLRG1), which is expressed by natural killer cells, memory T cells, and type 2 innate lymphoid cells. Engagement of KLRG1 by E-cadherin promotes inhibitory effects in the KLRG1-expressing cell, including inhibition of natural killer cell cytotoxicity, inhibition of antigen-induced proliferation, and induction of cytolytic activity of  $CD8^{+}$  T cells, and inhibition of type 2 cytokine production of type 2 innate lymphoid cells.<sup>41–43</sup> We speculate that CDH26 may act as a counter-regulatory molecule either through engagement of integrins or other unknown counter-receptors to dampen the Th2-associated inflammatory responses. Although molecules upregulated during disease might be

assumed to be involved in promoting disease, upregulation of CDH26 could be part of the mechanism by which resolution of inflammation occurs to promote the return of the tissue to homeostasis. Alternatively, it is possible that CDH26 engagement may inhibit particular subsets of  $CD4^{+}$  T cells: for example, regulatory T cells, which are known to be increased in EoE and EG,<sup>16,20,44</sup> or other more select  $CD4^{+}$  T-cell subsets such as Th1 or Th2 cells. Depending on the subset of T cells inhibited, the molecule could serve either to dampen or accelerate Th2-associated inflammatory responses. In summary, CDH26 is now the second CDH (besides CDH1) that has been shown to bind  $\alpha$ -integrins, extending the paradigm of CDH/integrin interactions and leading to the unexpected finding that CDH26-Fc (as well as CDH1-Fc) has T-cell immunosuppressive activity, providing a potential novel therapeutic strategy.

## METHODS

Methods related to patient studies, expression constructs, cell isolation, fluorescence-activated cell sorting analysis, enzyme-linked immunosorbent assay (ELISA), and bioinformatics analysis can be found in **Supplementary Material**.

### Quantitation of transcript levels

**Microarray analysis.** For microarray analysis, biopsy samples collected during the index endoscopy were stored in RNAlater until subjected to RNA isolation using the miRNeasy Kit (Qiagen, Germantown, MD) per the manufacturer's instructions. RNA labeling and hybridization to the GeneChip Human Genome U133 Plus 2.0 Array (Affymetrix, Santa Clara, CA) was performed as reported.<sup>26</sup> RNA labeling, hybridization, and generation of expression data were performed by the Gene Expression Microarray Core at Cincinnati Children's Hospital Medical Center (CCHMC), Cincinnati, Ohio, USA. In some cases, the raw signal intensity of particular probe sets was reported. Transcripts for which all individual samples exhibited a raw signal of  $\leq 100$  were considered to be not expressed. Transcripts with raw signal  $\geq 400$  were considered to be substantially expressed.

**Quantitative PCR.** Total RNA (100 ng–1  $\mu$ g) isolated from biopsy specimens using the miRNeasy Kit (Qiagen) or from cells using Trizol (Invitrogen, Waltham, MA) was used to synthesize cDNA using Superscript II Reverse Transcriptase (Invitrogen). Real-time PCR was performed using the iQ5 system (Bio-Rad, Hercules, CA) and SYBR green mix (Bio-Rad). The value obtained for each primer set (see **Supplementary Table S3**) was normalized to the *GAPDH* value for the corresponding sample.

### Protein and cell detection in tissue

**Histopathology.** Biopsies for histological evaluation were fixed in 10% formalin, routinely processed, and embedded in paraffin. Sections (5  $\mu$ m) were stained with hematoxylin and eosin or with specific antibodies. Immunohistochemical stains were performed using Ventana Benchmark XT automated immunostainer. Antigen retrieval (EDTA, 30 min) was followed by staining with anti-CDH26 (1:50, Sigma-Aldrich, St. Louis, MO) or anti-*H. pylori* (Ventana Medical Systems, Tuscon, AZ) antibodies. For quantitative microscopy, multiple levels of biopsies were surveyed, and the areas containing the greatest concentration of eosinophils or immunopositive cells were identified and enumerated at  $\times 400$  (0.3 mm<sup>2</sup>) to generate a peak count per biopsy. Quantitative evaluations were performed in well-oriented areas when feasible.

### Cell culture and manipulation

**Culture of cell lines and cytokine treatment.** Human esophageal squamous epithelial cancer cell line TE-7 was kindly provided by Dr Hainault (IARC, Lyon, France). These cells were maintained in RPMI medium (Invitrogen) supplemented with 5% fetal bovine serum (FBS);

Atlanta Biologicals, Flowery Branch, GA) and 1% penicillin/streptomycin (Invitrogen). HEK 293T cells and L929 cells were grown in Dulbecco's modified Eagle's medium (DMEM; Invitrogen) supplemented with 10% FBS (Atlanta Biologicals) and 1% penicillin/streptomycin (Invitrogen). Jurkat cells were cultured in RPMI medium (Invitrogen) supplemented with 10% FBS (Atlanta Biologicals) and 1% penicillin/streptomycin (Invitrogen).

**Lentivirus production and transduction of HEK 293T, TE-7, and L929 cells.** For pMIRNA1 constructs, lentivirus production was carried out by the CCHMC Viral Vector Core. HEK 293T, TE-7, and L929 cells were transduced by incubating lentivirus with the cells for 24 h in the presence of  $5 \mu\text{g ml}^{-1}$  polybrene. Media were then changed, and after 24 h, medium containing  $2 \mu\text{g ml}^{-1}$  puromycin was added. After selection for 48 h in puromycin, cells were dispersed and plated to single cells in 96-well plates to obtain clones derived from single cells. A second round of dispersing, plating to single cells, and picking single colonies was performed. CDH26 expression was verified by western blotting analysis.

### Protein methods

**Protein extracts and IP.** Cell lysates were prepared from HEK 293T cells generally as described. Cells (approximately  $2 \times 10^6$ ) were washed one time with phosphate-buffered saline and incubated in IP buffer (50 mM Tris-HCl (pH 7.4), 150 mM NaCl, 2 mM EDTA, 1 mM dithiothreitol, 1% Nonidet P-40 (NP-40); or 10 mM imidazole, 100 mM NaCl, 1 mM MgCl<sub>2</sub>, 5 mM EDTA, 1% Triton X-100, pH 7.4) containing  $1 \times$  complete protease inhibitor cocktail (Roche) for 10 min on ice. Cells were scraped from the plate and rotated at 4 °C for 10 min. Lysates were cleared by centrifugation at 20,000 g at 4 °C for 10 min. An equal amount of protein was added to total 500  $\mu\text{l}$  of IP buffer plus protease inhibitors (Roche). Antibodies (2  $\mu\text{g}$   $\alpha$ -HA (Covance, Princeton, NJ),  $\alpha$ -myc (Covance),  $\alpha$ -p120 (BD Transduction Laboratories, San Jose, CA),  $\alpha$ -ITGA4 (Cell Signaling Technology, Danvers, MA), mouse IgG1 control (AbD Serotec, Hercules, CA), or normal rabbit IgG control (R&D Systems, Minneapolis, MN)) were added and rotated overnight at 4 °C. Subsequently, 20  $\mu\text{l}$  of protein A/G agarose beads (Santa Cruz Biotechnology, Dallas, TX) were added per sample. After 2 h of rotation (4 °C), beads were washed five times in IP buffer containing protease inhibitors. In all,  $2 \times$  Laemmli buffer was added to the immunoprecipitates or total cell lysates saved prior to IP (input).

**Biopsy protein extracts.** Distal esophagus or gastric antrum biopsy specimens were transferred into 100  $\mu\text{l}$  of IP buffer (50 mM Tris-HCl (pH 7.4), 150 mM NaCl, 2 mM EDTA, 1 mM dithiothreitol, 1% Nonidet P-40 (NP-40),  $1 \times$  protease inhibitors (Roche)) and sonicated. Lysates were cleared by centrifugation (20,000 g, 4 °C, 10 min). Alternatively, protein was isolated from the organic fraction remaining after RNA isolation from biopsy specimens using the miRNeasy Kit (Qiagen). DNA was precipitated by the addition of 0.3 volumes of ethanol followed by a 2,000 g spin. Protein was precipitated from the supernatant by addition of three volumes of acetone, pelleted by centrifugation (20,000 g, 10 min, 4 °C), dried, and solubilized in Laemmli buffer ( $2 \times$ ).

**Biotinylation of cell surface proteins.** Adherent cells were washed with ice-cold biotinylation buffer (100 mM HEPES, 50 mM NaCl, pH 8.0) twice; cold biotinylation buffer plus sulfo-NHS-LC-biotin ( $0.9259 \text{ mg ml}^{-1}$ ) (Thermo Scientific) was then added (30 min on ice). Buffer was removed, cells were washed three times with ice-cold phosphate-buffered saline with 100 mM glycine, and protein was then extracted as described above using IP buffer with protease inhibitors. Cell lysates were incubated with streptavidin-agarose beads (Sigma-Aldrich) for 2 h at 4 °C. Beads were washed five times with cold IP buffer containing 1 mM PMSF followed by addition of  $2 \times$  Laemmli buffer.

**SDS-PAGE and western blotting analysis.** Total protein, inputs, or immunoprecipitates were loaded onto either 4–12% NuPage Tris-bis

gels (Invitrogen) and electrophoresed for 1.5 h at 150 V or 4–12% BOLT gels (Invitrogen) and electrophoresed for 50 min at 165 V. Proteins were then transferred to nitrocellulose membranes. Primary antibodies were diluted in TBS/0.1% Tween 20 containing 5% milk or Odyssey blocking buffer (LI-COR Biosciences, Lincoln, NE) + 0.2% Tween 20: rabbit anti-CDH26 (Sigma-Aldrich), 1:500; rabbit anti-beta-catenin (Cell Signaling Technology), 1:1,000; mouse anti-p120 (BD Transduction Laboratories), 1:1,000; mouse anti-HA (Covance), 1:1,000; rabbit anti-HA (Santa Cruz Biotechnology), 1:200; mouse anti-Myc (Cell Signaling Technology), 1:1,000; mouse anti-beta-actin (Sigma-Aldrich), 1:1,000; rabbit anti-V5 (Bethyl Laboratories), 1:1,000; rabbit anti-ITGA4 (Cell Signaling Technology), 1:1,000; and rabbit anti-E-cadherin (Cell Signaling Technology), 1:1,000. Horseradish peroxidase (HRP)-conjugated secondary antibodies were incubated with the membranes in TBS/0.1% Tween 20 containing 5% milk: anti-rabbit HRP, 1:10,000 (Cell Signaling Technology); anti-mouse HRP, 1:10,000 (Cell Signaling Technology). Blottings were developed using ECL Plus reagent (GE Healthcare, Chicago, IL). Densitometry measurements were performed using Multi Gauge V3.0 (Fugifilm, Valhalla, NY). Alternatively, secondary antibodies conjugated to infrared fluorophores (anti-rabbit IRDye 800CW or anti-mouse IRDye 680RD; 1:15,000) (LI-COR Biosciences) were used, and blotting was carried out in a similar manner except that antibodies were diluted in Odyssey blocking buffer (LI-COR Biosciences) + 0.2% Tween 20 and infrared signal was visualized and quantified using the Odyssey CLx Infrared Imaging System and ImageStudio software (LI-COR Biosciences).

**Solid phase adhesion assay.** Recombinant human integrin  $\alpha 4\beta 7$  (R&D Systems) was diluted to the indicated concentration in buffer (150 mM NaCl, 20 mM HEPES); 100  $\mu\text{l}$  per well was added to Costar half-well ELISA plates (Corning, Corning, NY) and incubated overnight at 4 °C. The following day, wells were washed and blocked with 5% BSA in buffer (150 mM NaCl, 20 mM HEPES) overnight at 4 °C. The following day, the wells were washed, and IgG1 or CDH26-IgG1-Fc diluted in assay buffer (150 mM NaCl, 20 mM HEPES, 1 mM CaCl<sub>2</sub>, 1 mM MgCl<sub>2</sub>, 1 mM MnCl<sub>2</sub>) containing 5% BSA was added to wells for 60 min at 37 °C. Wells were washed  $3 \times$ , and detection antibody (biotinylated anti-human IgG1 (Vector Laboratories, Burlingame, CA);  $0.5 \mu\text{g ml}^{-1}$  in assay buffer with 5% BSA) was added for 2 h at room temperature. Wells were washed  $3 \times$  with assay buffer with 5% BSA, and streptavidin-HRP was added (1:200 in assay buffer with 5% BSA; R&D Systems). Wells were washed  $3 \times$  with assay buffer with 5% BSA, and a 1:1 dilution of TMB substrate (BD Biosciences, San Jose, CA) was added. The reaction was stopped by the addition of  $2 \text{ N H}_2\text{SO}_4$ . Absorbance at 450 and 900 nm was measured using a plate reader (BioTek, Winooski, VT).

### Functional assays

**Aggregation assay.** L929 cells were treated with DMEM containing 0.1% trypsin at a final concentration of 5 mM CaCl<sub>2</sub> (30 min, 37 °C). Cells were washed once with DMEM containing 10% FBS and then twice with  $1 \times$  HBSS containing 1% FBS. Cells were counted, and  $2 \times 10^6$  cells were aliquoted into 1.5-ml tubes (two tubes per cell type). Cells were spun down and resuspended in HEPES-buffered magnesium-free saline (10 mM HEPES in saline) that either contained or lacked 1 mM CaCl<sub>2</sub>. The initial particle number was counted, and then tubes were rotated at 37 °C for 30 min. The final particle number was then counted. The aggregation index was expressed as ((initial particle number – final particle number)/initial particle number).

**Cell adhesion to recombinant integrin assay.** Recombinant human  $\alpha 4\beta 7$  (R&D Systems) was diluted to the indicated concentration in buffer (150 mM NaCl, 20 mM HEPES), and 100  $\mu\text{l}$  per well was added to half-well Costar ELISA plates (Corning) and incubated overnight at 4 °C. The following day, wells were washed and coated with 5% BSA in buffer (150 mM NaCl, 20 mM HEPES) (3 h, 37 °C). L929 cell clones transduced with the indicated construct and grown to confluency were then dispersed and resuspended in assay buffer (150 mM NaCl, 20 mM

HEPES, 1 mM CaCl<sub>2</sub>, 1 mM MgCl<sub>2</sub>, 1 mM MnCl<sub>2</sub>). For each cell type, 50,000 cells were added per well. The plate was spun at 10 g for 1 min and subsequently incubated at 37 °C for 1 h. Wells were washed by gravity one time by inverting the plate in a large beaker of assay buffer for 10 min. Two additional washes were performed by pipetting 100 µl of assay buffer into the wells four times per wash. Fluorescence was measured prior to the washes and after each wash using a plate reader (ex/em 485/20 nm/528/20 nm) (BioTek). The results are expressed as the percentage of fluorescence remaining (fluorescence after the last wash/initial fluorescence) for each well.

**Cell adhesion assay.** CDH26-hIgG1-Fc, CDH1-Fc (R&D Systems), and/or hIgG1 (Southern Biotech, Birmingham, AL) were diluted in buffer (150 mM NaCl, 20 mM HEPES) to appropriate concentrations so that the indicated amount of protein was added to Costar half-well ELISA plates in 50 µl per well (Corning) and incubated overnight at 4 °C. The next day, Jurkat cells ( $1 \times 10^6$  ml<sup>-1</sup>) were incubated in HEPES medium (132 mM NaCl, 6 mM KCl, 1 mM CaCl<sub>2</sub>, 1 mM MgSO<sub>4</sub>, 1.2 mM KH<sub>2</sub>PO<sub>4</sub>, 20 mM HEPES, 5.5 mM glucose, 0.5% BSA) plus 4 µg ml<sup>-1</sup> calcein-AM (Sigma-Aldrich) for 1 h at 37 °C. Cells were washed 3 × in HEPES medium. In the indicated cases, cells were incubated with 1.4 µg of either anti-integrin β1-activating antibodies (clone TS2/16, Santa Cruz Biotechnology) or an equivalent amount of mIgG1 (Southern Biotech). In the indicated cases, labeled cells were then preincubated with the indicated amount of either mIgG1 (AbD Serotec), anti-integrin α4 (HP2/1; AbD Serotec), or anti-CD32 (Stem Cell Technologies, Vancouver, BC, Canada) antibodies in assay buffer for non-TS2/16-treated cells (150 mM NaCl, 10 mM HEPES, 1 mM CaCl<sub>2</sub>, 1 mM MgCl<sub>2</sub>, 1 mM MnCl<sub>2</sub>) or HEPES medium for TS2/16-treated cells for 15 min at 4 °C prior to their addition to wells (50,000 cells per well). Plates were spun at 10 g for 1 min and then incubated at 37 °C for 45 min. Initial fluorescence per well was then measured using a plate reader ((ex/em 360/40 nm/460/40 nm); BioTek). Wells were washed by gravity one time by inverting the plate in a large beaker of assay buffer for 10 min. Two additional washes were performed by pipetting 100 µl of assay buffer into the wells four times per wash. Final fluorescence was then measured.

**CD4<sup>+</sup> T-cell activation assay.** The indicated amounts of anti-CD3 (clone OKT3, eBioscience, San Diego, CA) antibodies, CDH26-hIgG1-Fc, CDH1-Fc (R&D Systems), and/or hIgG1 control antibody (Southern Biotech) were suspended in coating buffer (20 mM HEPES, 150 mM NaCl), added to wells of a 96-well cell culture plate, and incubated overnight at 4 °C. The following day, isolated human peripheral blood CD4<sup>+</sup> T cells (150,000 per well) were added to the wells in RPMI supplemented with 10% FBS, 1% penicillin/streptomycin, and 200 mM glutamine. Cells were incubated for 48 h. Cells and supernatants were then collected for analysis by flow cytometry and ELISA, respectively.

**Statistics.** Data are expressed as mean ± s.e.m. or median ± interquartile range. Statistical significance was determined using unpaired *t*-test (2 groups, normal distribution, equal variance), Mann-Whitney test (2 groups, nonparametric), one-way analysis of variance followed by the Tukey's posttest (> 2 groups), or the Kruskal-Wallis test followed by Dunn's multiple comparison test (> 2 groups, nonparametric) with the Prism 5.0 software (GraphPad Software, La Jolla, CA).

**SUPPLEMENTARY MATERIAL** is linked to the online version of the paper at <http://www.nature.com/mi>

#### ACKNOWLEDGMENTS

We thank the CCED and clinical research coordinators for facilitating patient sample and data collection; Michael Eby for EGID database maintenance, queries, and retrieval of patient information; the Cincinnati Digestive Health Center Integrative Morphology Core for tissue processing, sectioning, histology, and immunohistochemical staining; Betsy DiPasquale for assistance with immunohistochemical stains; Dr Andrew Herr for

advice regarding protein expression and purification; Dr Bruce Bochner for critical review of the manuscript; and physicians who collected biopsy samples, including Dr James Franciosi, Dr Kathleen Campbell, Dr Michael Farrell, Dr Ajay Kaul, and Dr Gitit Tomer. This work was supported in part by NIH U19 AI070235, NIH R01 DK076893, the PHS Grant P30 DK0789392, American Heart Association 11POST440046, the Sunshine Charitable Foundation and its supporters, Denise A. Bunning and David G. Bunning, the Buckeye Foundation, and the Campaign Urging Research for Eosinophilic Diseases (CURED) Foundation.

#### AUTHOR CONTRIBUTIONS

J.M.C. and M.H.C. designed and performed experiments, analyzed data, and wrote the paper; K.A.K. performed tissue sample processing and performed experiments; J.D.S., T.W., M.R., L.A., and H.T. designed and performed experiments and analyzed data; M.J.D., M.R.W., and A.P. performed protein structure and bioinformatics analyses and gave conceptual advice; E.M.S. performed tissue sample processing and assisted in acquiring clinical information; P.E.P. collected patient tissue; J.P.A. acquired clinical information and gave conceptual advice; M.E.R. designed the study, analyzed data, and wrote the paper.

#### DISCLOSURE

M.E.R. is a consultant for Receptos, Pulm-One, and NKT Therapeutics and has an equity interest in Immune Pharmaceuticals, Pulm-One, and NKT Therapeutics and royalties in reslizumab (Teva Pharmaceuticals). M.H.C. is a consultant for Meritage Pharma, Novartis, Receptos, Regeneron, and Aptalis. J.M.C. and M.E.R. are co-inventors of patents and/or applications, owned by Cincinnati Children's Hospital, concerning some of the data in this paper. The other authors declared no conflict of interest.

© 2017 Society for Mucosal Immunology

#### REFERENCES

- Shimoyama, Y. *et al.* Cadherin cell-adhesion molecules in human epithelial tissues and carcinomas. *Cancer Res.* **49**, 2128–2133 (1989).
- Wheelock, M.J., Shintani, Y., Maeda, M., Fukumoto, Y. & Johnson, K.R. Cadherin switching. *J. Cell. Sci.* **121** (Pt 6), 727–735 (2008).
- Gassler, N. *et al.* Inflammatory bowel disease is associated with changes of enterocytic junctions. *Am. J. Physiol. Gastrointest. Liver Physiol.* **281**, G216–G228 (2001).
- Heijink, I.H., Nawijn, M.C. & Hackett, T.L. Airway epithelial barrier function regulates the pathogenesis of allergic asthma. *Clin. Exp. Allergy* **44**, 620–630 (2014).
- Hupin, C., Gohy, S., Bouzin, C., Lecocq, M., Polette, M. & Pilette, C. Features of mesenchymal transition in the airway epithelium from chronic rhinosinusitis. *Allergy* **69**, 1540–1549 (2014).
- Trautmann, A. *et al.* The differential fate of cadherins during T-cell-induced keratinocyte apoptosis leads to spongiosis in eczematous dermatitis. *J. Invest. Dermatol.* **117**, 927–934 (2001).
- Valencia, X. *et al.* Cadherin-11 provides specific cellular adhesion between fibroblast-like synoviocytes. *J. Exp. Med.* **200**, 1673–1679 (2004).
- Trautmann, A. *et al.* Apoptosis and loss of adhesion of bronchial epithelial cells in asthma. *Int. Arch. Allergy Immunol.* **138**, 142–150 (2005).
- de Boer, W.I., Sharma, H.S., Baelemans, S.M., Hoogsteden, H.C., Lambrecht, B.N. & Braunstahl, G.J. Altered expression of epithelial junctional proteins in atopic asthma: possible role in inflammation. *Can. J. Physiol. Pharmacol.* **86**, 105–112 (2008).
- Heijink, I.H., Kies, P.M., Kauffman, H.F., Postma, D.S., van Oosterhout, A.J. & Vellenga, E. Down-regulation of E-cadherin in human bronchial epithelial cells leads to epidermal growth factor receptor-dependent Th2 cell-promoting activity. *J. Immunol.* **178**, 7678–7685 (2007).
- Cepek, K.L., Parker, C.M., Madara, J.L. & Brenner, M.B. Integrin alpha E beta 7 mediates adhesion of T lymphocytes to epithelial cells. *J. Immunol.* **150** (8 Pt 1), 3459–3470 (1993).
- Cepek, K.L. *et al.* Adhesion between epithelial cells and T lymphocytes mediated by E-cadherin and the alpha E beta 7 integrin. *Nature* **372**, 190–193 (1994).



13. Schon, M.P. *et al.* Mucosal T lymphocyte numbers are selectively reduced in integrin alpha E (CD103)-deficient mice. *J. Immunol.* **162**, 6641–6649 (1999).
14. Uchida, Y., Kawai, K., Ibusuki, A. & Kanekura, T. Role for E-cadherin as an inhibitory receptor on epidermal gammadelta T cells. *J. Immunol.* **186**, 6945–6954 (2011).
15. Teitelbaum, J.E. *et al.* Eosinophilic esophagitis in children: immunopathological analysis and response to fluticasone propionate. *Gastroenterology* **122**, 1216–1225 (2002).
16. Tantibhaedhyangkul, U., Tatevian, N., Gilger, M.A., Major, A.M. & Davis, C.M. Increased esophageal regulatory T cells and eosinophil characteristics in children with eosinophilic esophagitis and gastroesophageal reflux disease. *Ann. Clin. Lab. Sci.* **39**, 99–107 (2009).
17. Lucendo, A.J. *et al.* Immunophenotypic characterization and quantification of the epithelial inflammatory infiltrate in eosinophilic esophagitis through stereology: an analysis of the cellular mechanisms of the disease and the immunologic capacity of the esophagus. *Am. J. Surg. Pathol.* **31**, 598–606 (2007).
18. Doherty, T.A. *et al.* Group 2 innate lymphocytes (ILC2) are enriched in active eosinophilic esophagitis. *J. Allergy Clin. Immunol.* **136**, 792–794 e793 (2015).
19. Blanchard, C. *et al.* IL-13 involvement in eosinophilic esophagitis: transcriptome analysis and reversibility with glucocorticoids. *J. Allergy Clin. Immunol.* **120**, 1292–1300 (2007).
20. Caldwell, J.M. *et al.* Histologic eosinophilic gastritis is a systemic disorder associated with blood and extragastric eosinophilia, TH2 immunity, and a unique gastric transcriptome. *J. Allergy Clin. Immunol.* **134**, 1114–1124 (2014).
21. Bochner, B.S. Road signs guiding leukocytes along the inflammation superhighway. *J. Allergy Clin. Immunol.* **106**, 817–828 (2000).
22. Woodruff, P.G. *et al.* Genome-wide profiling identifies epithelial cell genes associated with asthma and with treatment response to corticosteroids. *Proc. Natl. Acad. Sci. USA* **104**, 15858–15863 (2007).
23. Shum, B.O. *et al.* The adipocyte fatty acid-binding protein aP2 is required in allergic airway inflammation. *J. Clin. Invest.* **116**, 2183–2192 (2006).
24. Zhen, G. *et al.* IL-13 and epidermal growth factor receptor have critical but distinct roles in epithelial cell mucin production. *Am. J. Respir. Cell Mol. Biol.* **36**, 244–253 (2007).
25. Li, R.W. & Gasbarre, L.C. A temporal shift in regulatory networks and pathways in the bovine small intestine during *Cooperia oncophora* infection. *Int. J. Parasitol.* **39**, 813–824 (2009).
26. Blanchard, C. *et al.* Eotaxin-3 and a uniquely conserved gene-expression profile in eosinophilic esophagitis. *J. Clin. Invest.* **116**, 536–547 (2006).
27. Ikuse, T. *et al.* Microarray analysis of gastric mucosa among children with *Helicobacter pylori* infection. *Pediatr. Int.* **54**, 319–324 (2012).
28. Wen, S., Felley, C.P., Bouzourene, H., Reimers, M., Michetti, P. & Pan-Hammarstrom, Q. Inflammatory gene profiles in gastric mucosa during *Helicobacter pylori* infection in humans. *J. Immunol.* **172**, 2595–2606 (2004).
29. Truong, K. & Ikura, M. The cadherin superfamily database. *J. Struct. Funct. Genomics* **2**, 135–143 (2002).
30. Shapiro, L. & Weis, W.I. Structure and biochemistry of cadherins and catenins. *Cold Spring Harb. Perspect. Biol.* **1**, a003053 (2009).
31. Stappert, J. & Kemler, R. A short core region of E-cadherin is essential for catenin binding and is highly phosphorylated. *Cell Adhes. Commun.* **2**, 319–327 (1994).
32. Jou, T.S., Stewart, D.B., Stappert, J., Nelson, W.J. & MARRS, J.A. Genetic and biochemical dissection of protein linkages in the cadherin-catenin complex. *Proc. Natl. Acad. Sci. USA* **92**, 5067–5071 (1995).
33. Whittard, J.D. *et al.* E-cadherin is a ligand for integrin alpha2beta1. *Matrix Biol.* **21**, 525–532 (2002).
34. Taraszka, K.S., Higgins, J.M., Tan, K., Mandelbrot, D.A., Wang, J.H. & Brenner, M.B. Molecular basis for leukocyte integrin alpha(E)beta(7) adhesion to epithelial (E)-cadherin. *J. Exp. Med.* **191**, 1555–1567 (2000).
35. Seminario, M.C., Sterbinsky, S.A. & Bochner, B.S. Beta 1 integrin-dependent binding of Jurkat cells to fibronectin is regulated by a serine-threonine phosphatase. *J. Leukoc. Biol.* **64**, 753–758 (1998).
36. Lehnert, K., Print, C.G., Yang, Y. & Krissansen, G.W. MAdCAM-1 costimulates T cell proliferation exclusively through integrin alpha4beta7, whereas VCAM-1 and CS-1 peptide use alpha4beta1: evidence for "remote" costimulation and induction of hyperresponsiveness to B7 molecules. *Eur. J. Immunol.* **28**, 3605–3615 (1998).
37. van Seventer, G.A. *et al.* Analysis of T cell stimulation by superantigen plus major histocompatibility complex class II molecules or by CD3 monoclonal antibody: costimulation by purified adhesion ligands VCAM-1, ICAM-1, but not ELAM-1. *J. Exp. Med.* **174**, 901–913 (1991).
38. Shimizu, Y., van Seventer, G.A., Horgan, K.J. & Shaw, S. Costimulation of proliferative responses of resting CD4+ T cells by the interaction of VLA-4 and VLA-5 with fibronectin or VLA-6 with laminin. *J. Immunol.* **145**, 59–67 (1990).
39. Abonia, J.P. *et al.* Involvement of mast cells in eosinophilic esophagitis. *J. Allergy Clin. Immunol.* **126**, 140–149 (2010).
40. Berg, R.W., Yang, Y., Lehnert, K. & Krissansen, G.W. Mouse M290 is the functional homologue of the human mucosal lymphocyte integrin HML-1: antagonism between the integrin ligands E-cadherin and RGD tripeptide. *Immunol. Cell Biol.* **77**, 337–344 (1999).
41. Grundemann, C. *et al.* Cutting edge: identification of E-cadherin as a ligand for the murine killer cell lectin-like receptor G1. *J. Immunol.* **176**, 1311–1315 (2006).
42. Salimi, M. *et al.* A role for IL-25 and IL-33-driven type-2 innate lymphoid cells in atopic dermatitis. *J. Exp. Med.* **210**, 2939–2950 (2013).
43. Ito, M., Maruyama, T., Saito, N., Koganei, S., Yamamoto, K. & Matsumoto, N. Killer cell lectin-like receptor G1 binds three members of the classical cadherin family to inhibit NK cell cytotoxicity. *J. Exp. Med.* **203**, 289–295 (2006).
44. Fuentebella, J. *et al.* Increased number of regulatory T cells in children with eosinophilic esophagitis. *J. Pediatr. Gastroenterol. Nutr.* **51**, 283–289 (2010).